Spectral Mapping

The industry standard for portable Short wavelength Infrared spectrometers is the ASD “Terra Spec”. SWIR mapping is ideally suited for clay mineralogy and low temperature hydrothermal systems. In higher temperature systems, where the alteration minerals contain fewer OH groups, the spectral signatures are not so distinctive. In theory, biotite should give distinctive spectral signatures, but in practice, the absorption features in biotite are quite weak, and because of the low signal to noise ratio the wavelength shifts in the biotite cannot be accurately measured.

Consider the list of minerals in porphyry systems that can be mapped with SWIR; biotite (solid solutions), amphibole (hornblende, actinolite), epidote (epidote to clinozoisite solid solution is mappable), sericite (solid solutions), chlorite (solid solutions), kaolinite, alunite, pyrophyllite, etc. Of these, the mineral that is most widespread, easily measured and with significant solid solution variations is sericite. The distribution of sericite and the solid solution variations within it potentially provide a great vectoring tool for mapping zonations within lithocap environments.

Figure 1 demonstrates the effect of solid solution chemistry on white mice spectra by comparing two different spectra on the same plot. This plot shows the variation that can be measured from the characteristic mica absorption feature around 2200nm. The wavelength at the minimum point for this feature can shift between 2185 to 2225nm.

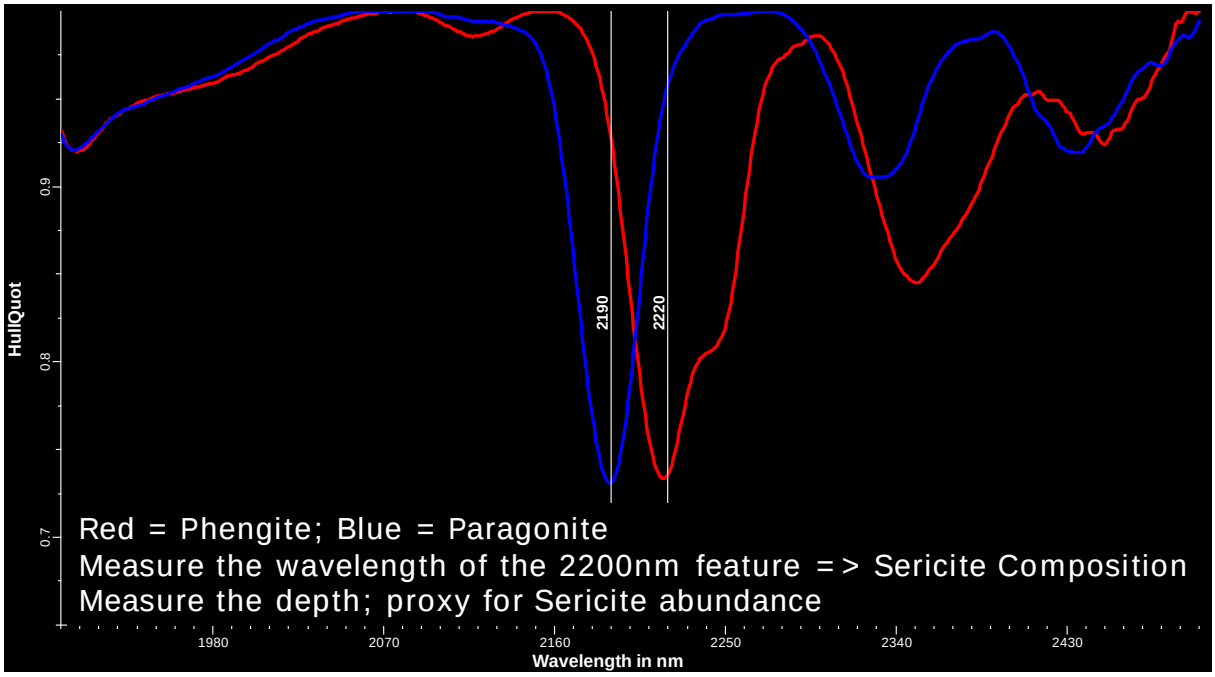

Figure 1.

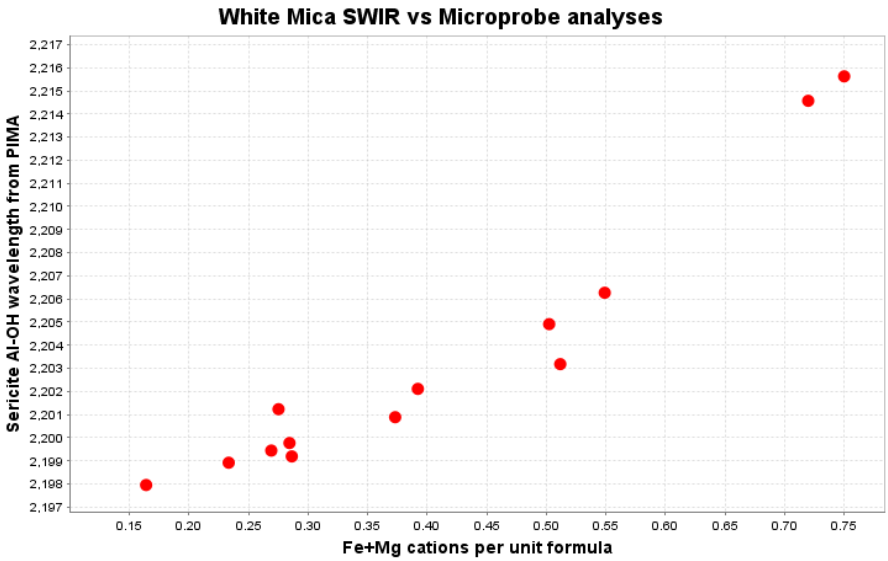

Fe+Mg cations per unit formula; $K_2(Al,Fe,Mg)_4(Al,Si)_8O_{20}(OH)_4$

Figure 2.

Figure 2 shows the reason for the wavelength shift. This is a data set where EMP analyses of white micas are plotted against the wavelength at the minimum point from the SWIR spectra. The shift in the wavelength is correlated with substitution of Mg and/or Fe for Al in the mica structure.

Drill Hole MJ024
Wavelength of 2200nm absorption feature in sericite, plotted against depth down hole

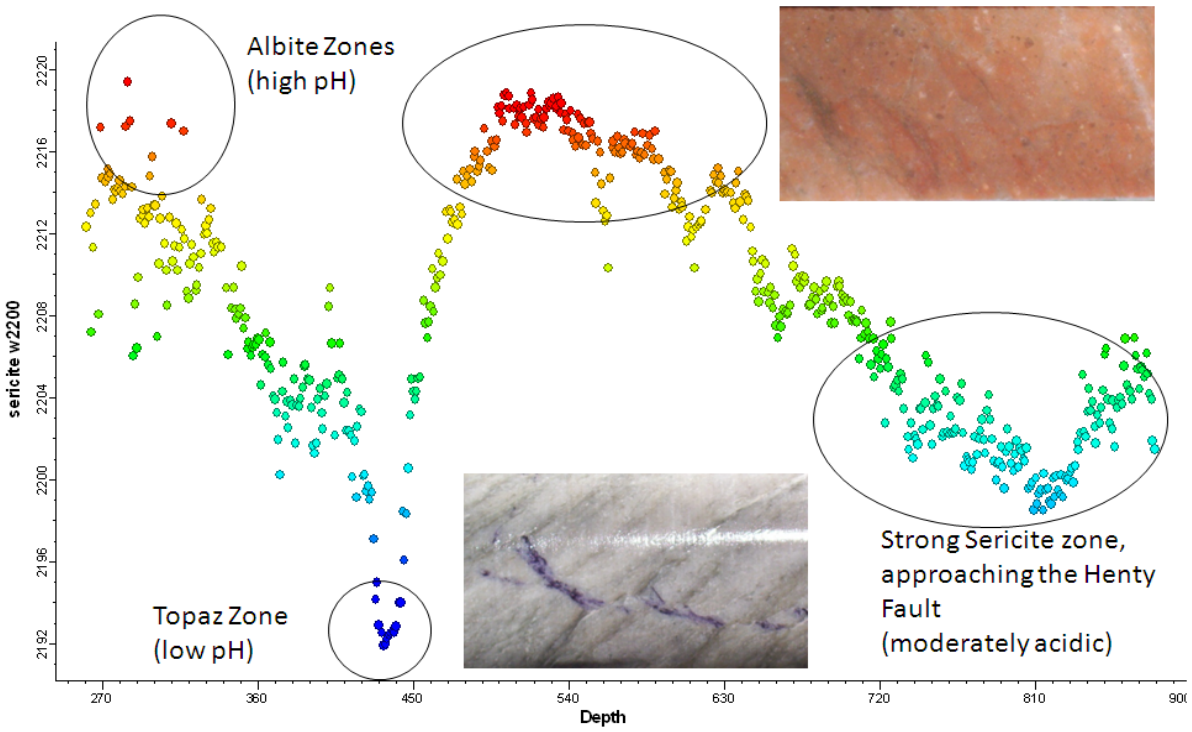

$2KAl_2(AlSi_3)O_{10}(OH)_2$ (musc) + K^+ + $1.5Fe^{2+}$ +$4.5SiO_2$ +$3H_2O$ ⇔ $3KFe_{0.5}Al_2(Al_{0.5}Si_{3.5})O_{10}(OH)_2$ (phen) + $4H^+$

The muscovite to phengite reaction is controlled by pH.
Muscovite means acid fluid; phengite means alkaline fluid.
The shift in the white mica wavelength can be used as a hydrothermal pH indicator.

Figure 3.

Figure 3 shows spectral data from drill hole MJ024 from Henty. Wavelength of 2200nm absorption feature in sericite, plotted against depth down hole. Very short wawelength micas occur where there is an advanced argillic assemblage of topaz, dickite, pyrophyllite and fluorite. In contrast, albite-rich alteration zones (alkaline) have very long mica wavelengths. In this case, the shift in the wavelength is a proxy for the pH in the hydrothermal system. The rule of thumb is; feldspar-destructive alteration produces short wavelength white mica. Where abundant new hydrothermal feldspar is formed, the white mica has very long wavelengths, (usually >2215nm). At low W/R ratios, or rock-buffered environments, wavelengths are intermediate 2205-2210nm.

Spectral Patterns in Porphyry Copper Deposits

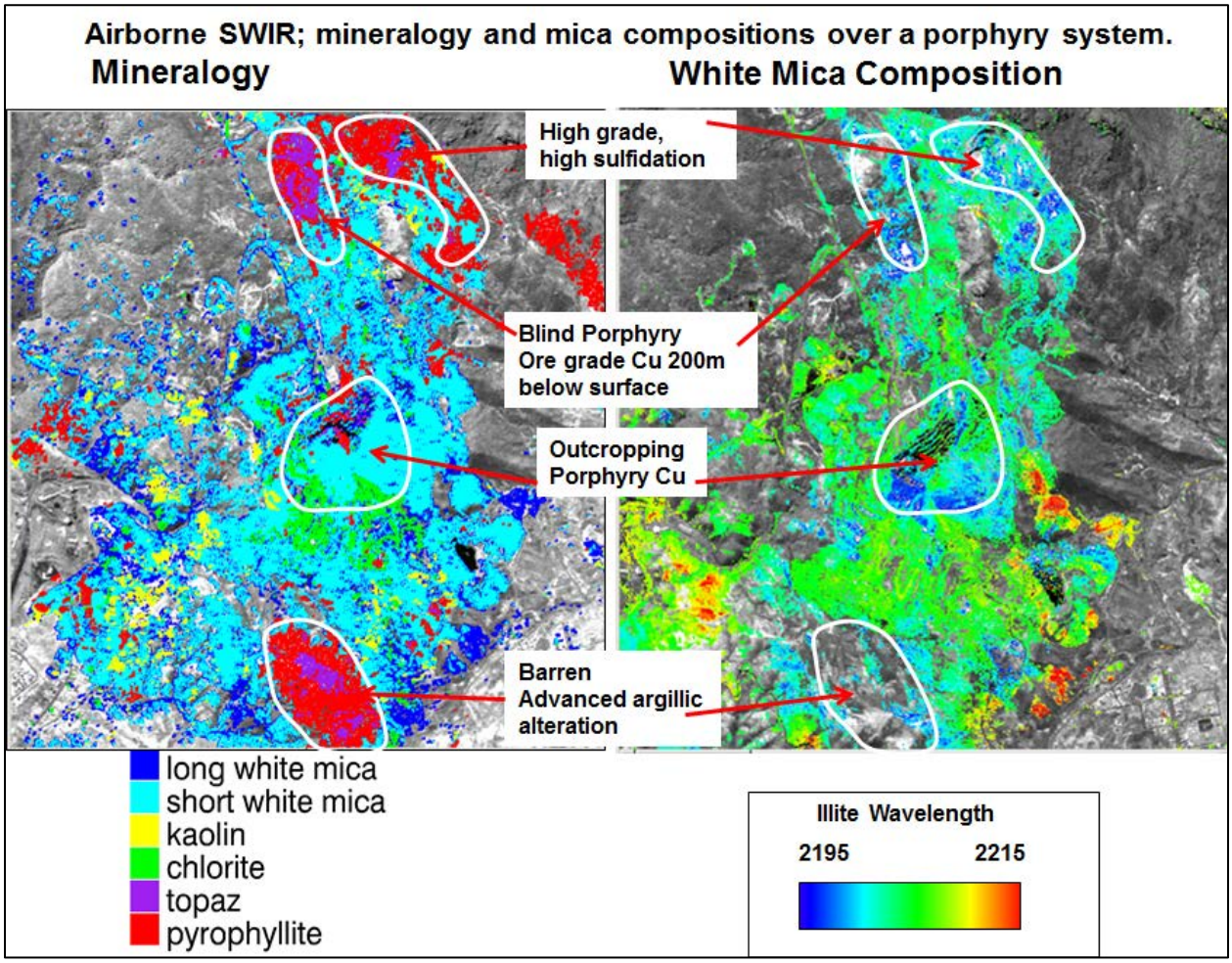

Figure 4. HyMap imagery over a porphyry copper system (Mount Lyell). The image on the left shows mineralogy. The image on the right is coloured by the wavelength of the 2200nm feature for all the pixels that contain white mica.

An airborne hyperspectral survey over a porphyry copper system is shown in figure 4. The image on the left shows the mineralogy. In the image on the right, all the pixels that have a white mica signature have been coloured by the wavelength of the Al-OH feature. The zones of advanced argillic alteration (topaz, pyrophyllite) occur above the top of blind porphyry copper fingers. Surrounding the zones of advanced argillic alteration, the Al-OH feature in the white mica shifts to shorter wavelengths. It can be seen from figure 15 that Cu mineralization is likely to be directly under the advanced argillic alteration, but in the absence of an advanced argillic cap, the target is to drill beneath the zone of shortest wavelength white mica. This is shown schematically in figure 5.

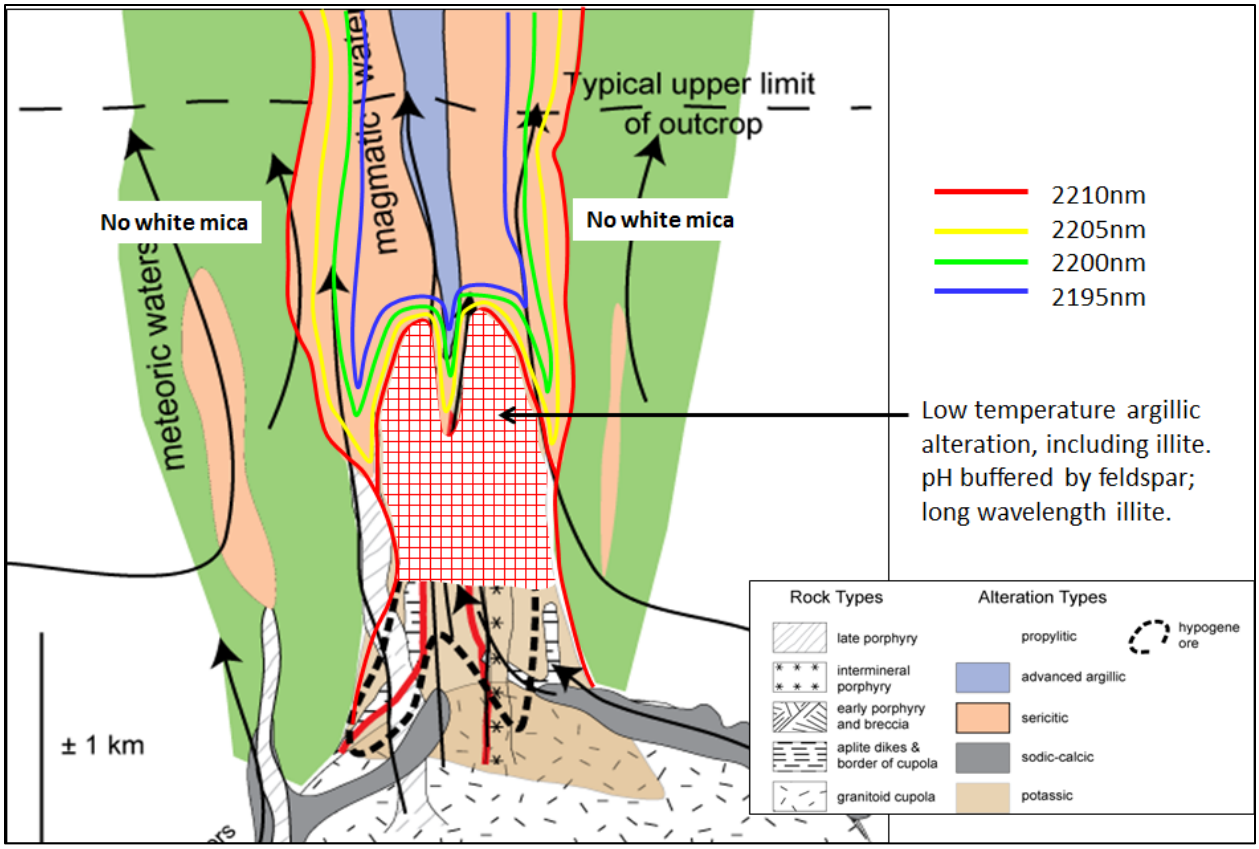

Figure 5. Schematic model of white mica SWIR wavelengths above a porphyry copper system.

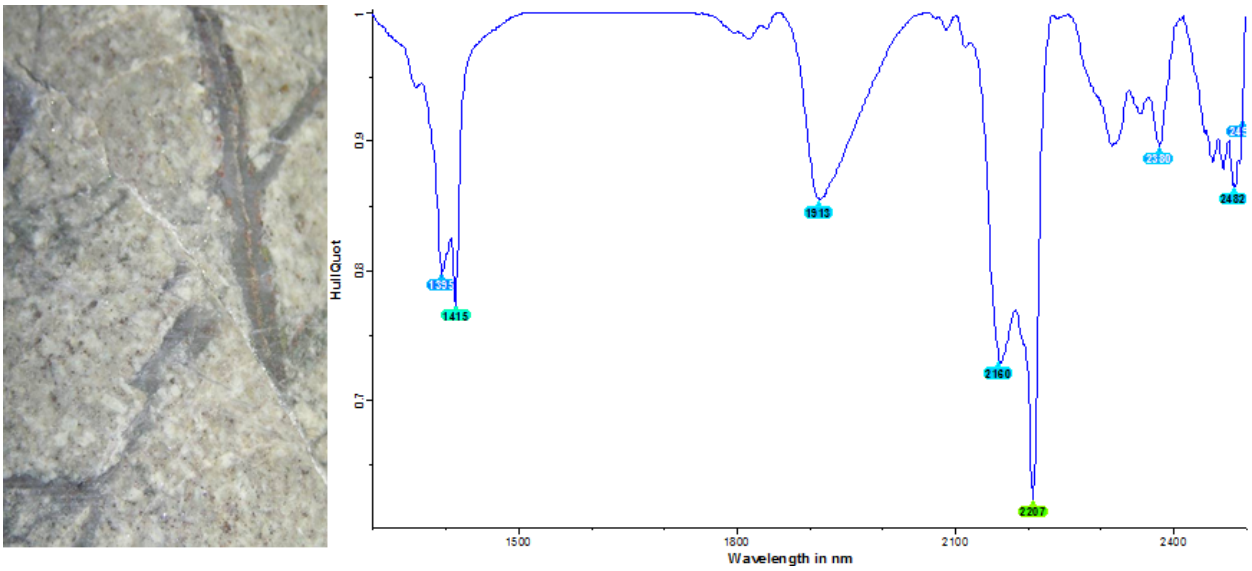

Figure 6. Hypogene kaolinite overprinting potassic alteration at Red Chris.

A surprising outcome of ASD mapping is how common and how extensive overprinting low temperature alteration is within the central cores of the PCD's. The central part of a PCD generally remains as a fluid pathway right through the waning stages of the hydrothermal system. This appears to be the result of magmatic fluid continuing to be expelled from the parental magma chamber until the whole system has cooled to ambient temperatures. Feldspars are very susceptible to hydrolysis reactions at low temperatures. Zones that were feldspar-stable at high temperatures show the most abundant evidence of overprinting. SWIR mapping is very sensitive to even very small amounts of clay minerals, and the overprinting may just amount to a cloudy dusting in the feldspars. Nevertheless this will be enough to give a significant spectral response. The overprinting minerals are generally smectitic clays, but in many locations, the retrograde mineralogy will also include illite or kaolinite. Where white micas were formed during earlier high temperature alteration, they are relatively resistant to overprinting by the lower temperature assemblages (white micas are also the last mineral to be overprinted by supergene clays in a weathering profile). An example of this is shown in figure 6. This shows kaolinite overprinting potassic alteration at 700m depth within the Red Chris porphyry in British Columbia.

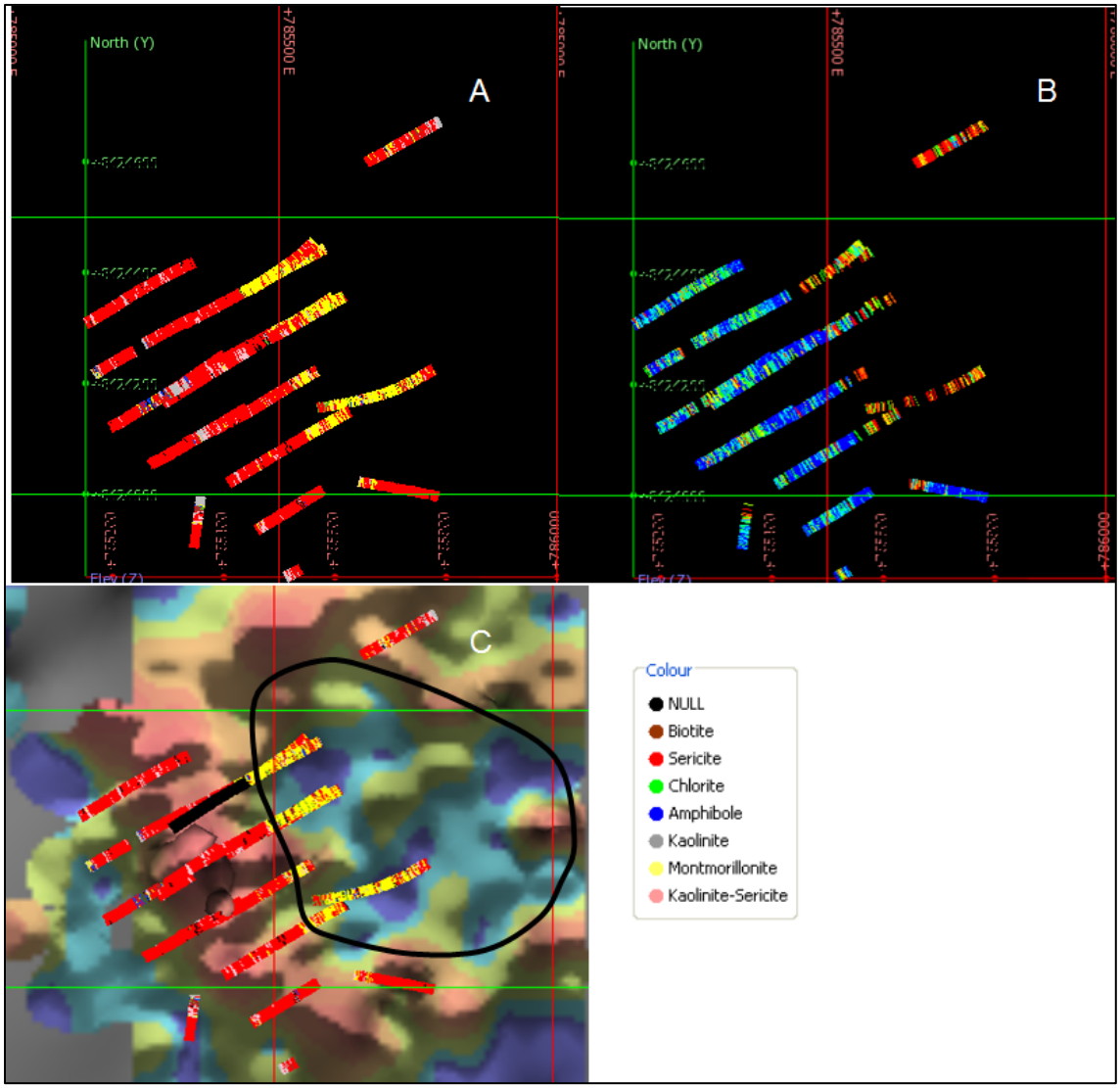

Figure 7. (a) SWIR mineralogy from a porphyry Cu system plotted as down hole strings; (b) wavelength of white micas; Blue < 2198nm, Red > 2208 nm; (c) SWIR mineralogy, overlain on surface geochemistry, showing a classic porphyry Cu moly donut.

Figure 7 shows an example of the SWIR mineralogy in a 3D data set. This shows pervasive muscovite in a phyllic alteration halo, whilst the potassic core of the system reports in the SWIR data as a zone of montmorillonite. The wavelengths of the sericite in the phyllic halo are all less than 2198nm. Some of the retrograde alteration includes illite. This has formed at relatively low water to rock ratios in feldspar rich rocks, hence the micas have relatively long 2200nm features. Figure 18c shows the down hole ASD mineralogy plotted relative to surface molybdenum geochemistry. The surface geochem shows a classic moly halo surrounding the potassic core. This clearly shows the correlation of smectite with the core of the porphyry.

Garfield ASD Results

The ASD spectra were classified according to the dominant mineralogy. They were divided into the following categories;

- Sericite
- Chlorite
- Mixed sericite-chlorite
- Kaolinite
- Mixed kaolinite-sericite

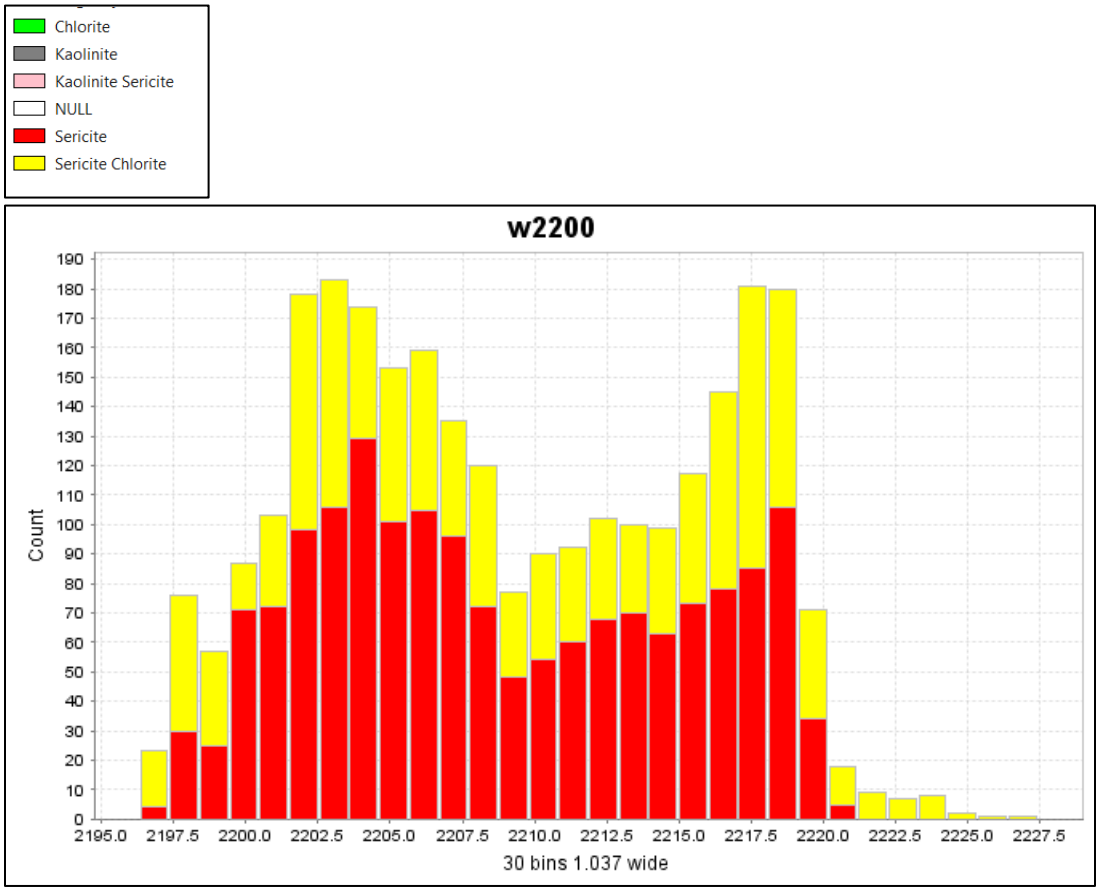

Figure 8. Wavelength at the minimum point of the 2200nm feature for all white-mica bearing spectra from Garfield.

For all the samples containing sericite or sericite-chlorite, the wavelength of the 2200nm feature was extracted and added to a column called “Sericite Composition”. A histogram of these values is shown in figure 8.

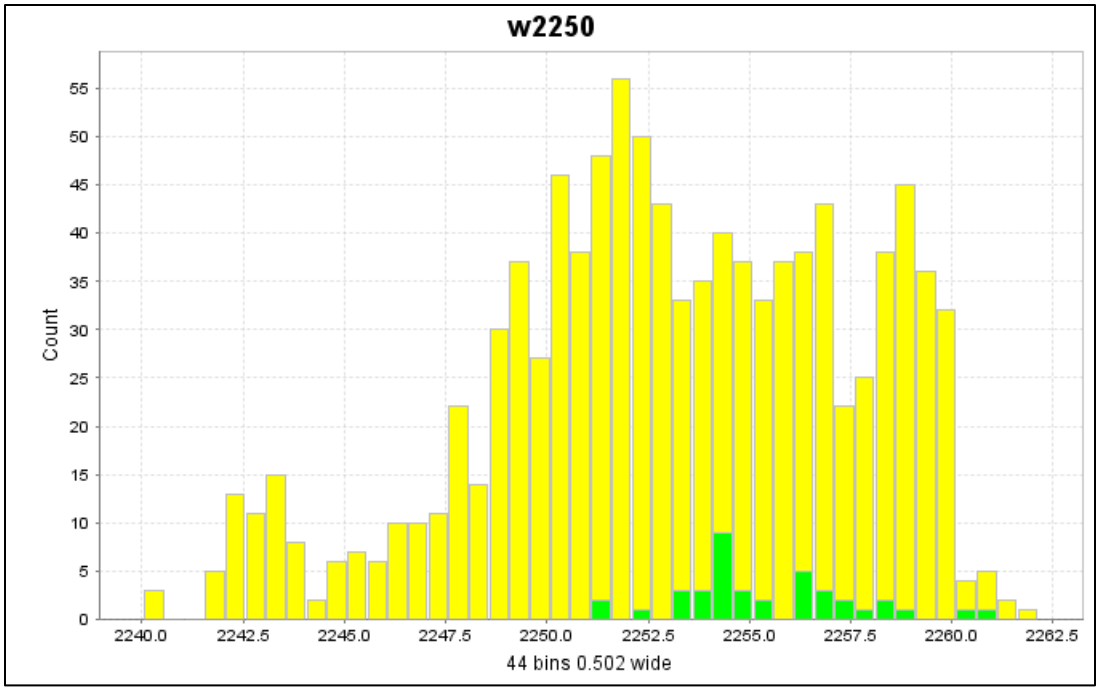

Figure 9. Wavelength at the minimum point of the 2250nm feature for all chlorite-mica bearing spectra from Garfield.

For all the samples containing chlorite or sericite-chlorite, the wavelength of the 2250nm feature was extracted and added to a column called “Chlorite Composition”. A histogram of these values is shown in figure 9.

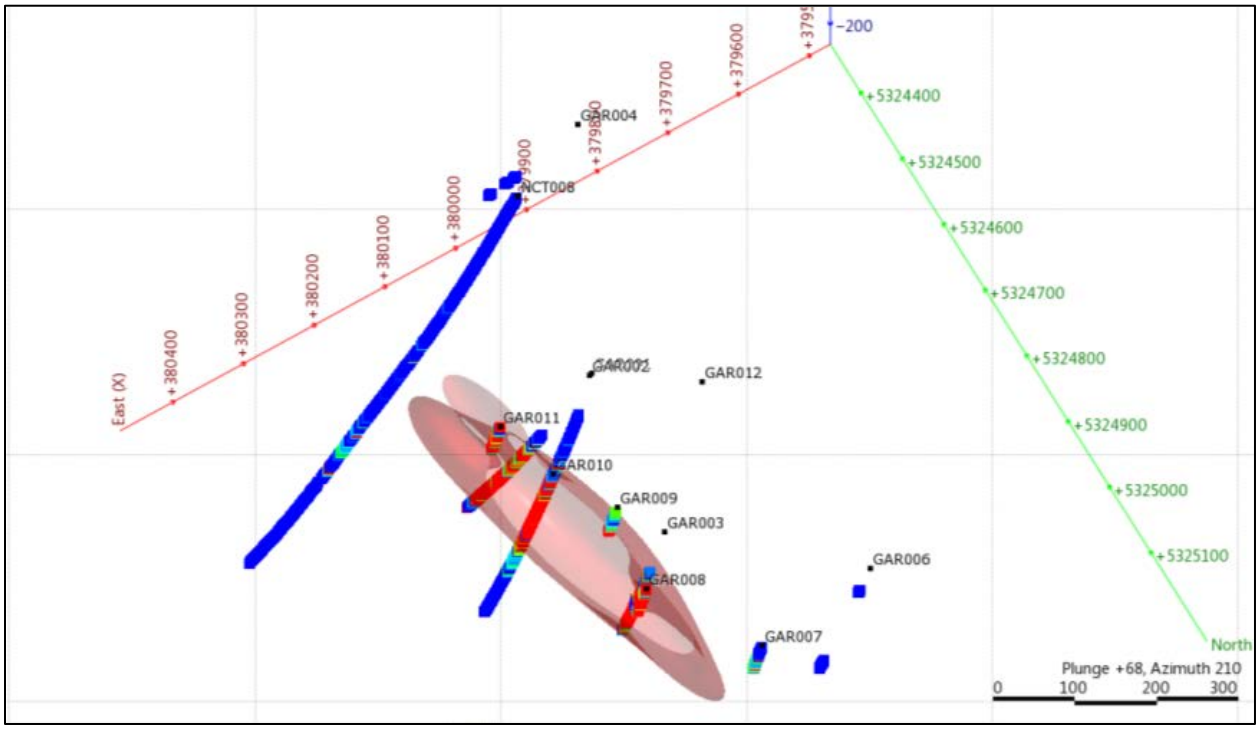

Figure 10. Copper assays; blue<100ppm, red>1000ppm. The red shape shows an isoshell of Cu>0.1%.

A simple iso-shell of copper grades greater than 0.1% was generated to act as a reference for the spectral data (figure 10).

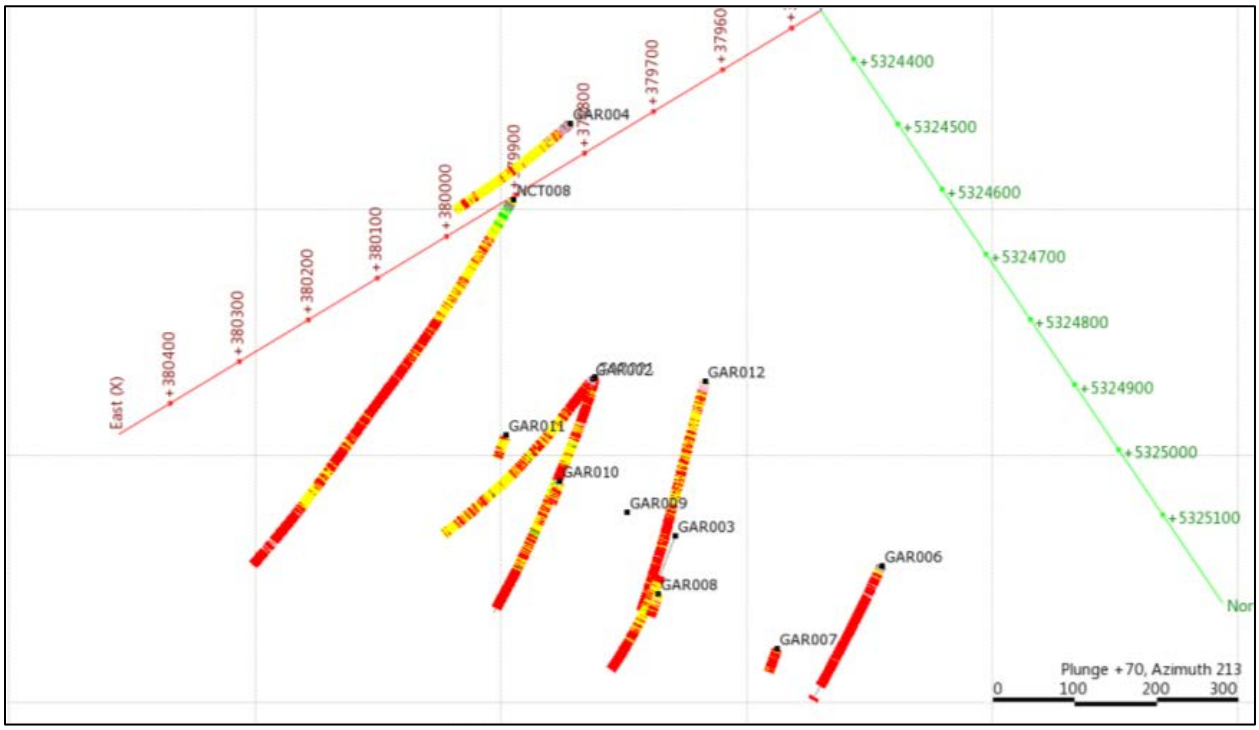

Figure 11. Down hole ASD mineralogy from the same field of view as figure 10.

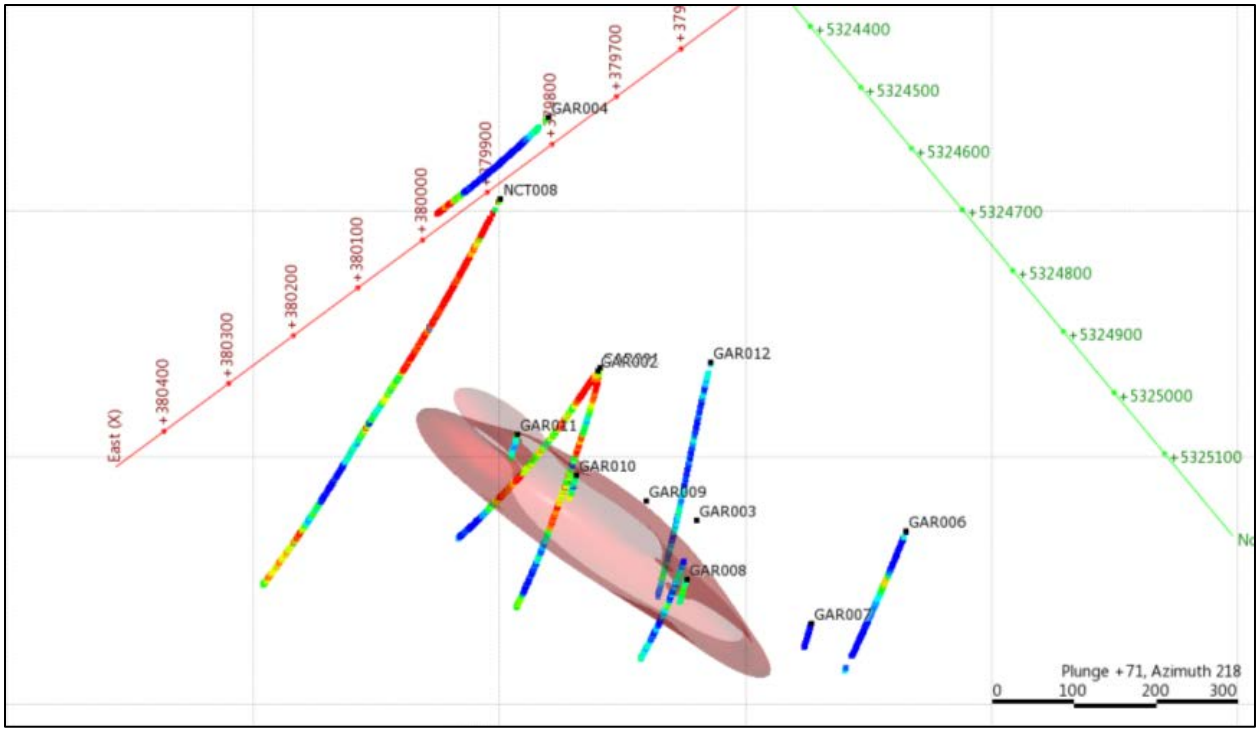

Figure 12. Down hole white mica compositions; blue<2200nm, red>2218nm. The red shape is Cu>0.1%.

The sericite compositions within the best mineralized parts of Garfield are strongly phengitic. White micas in the surrounding alteration halo are muscovitic (acid signature). This is very much like the example shown in figure 7, and matches the pattern described by Kim Denwer from Prince Lyell.

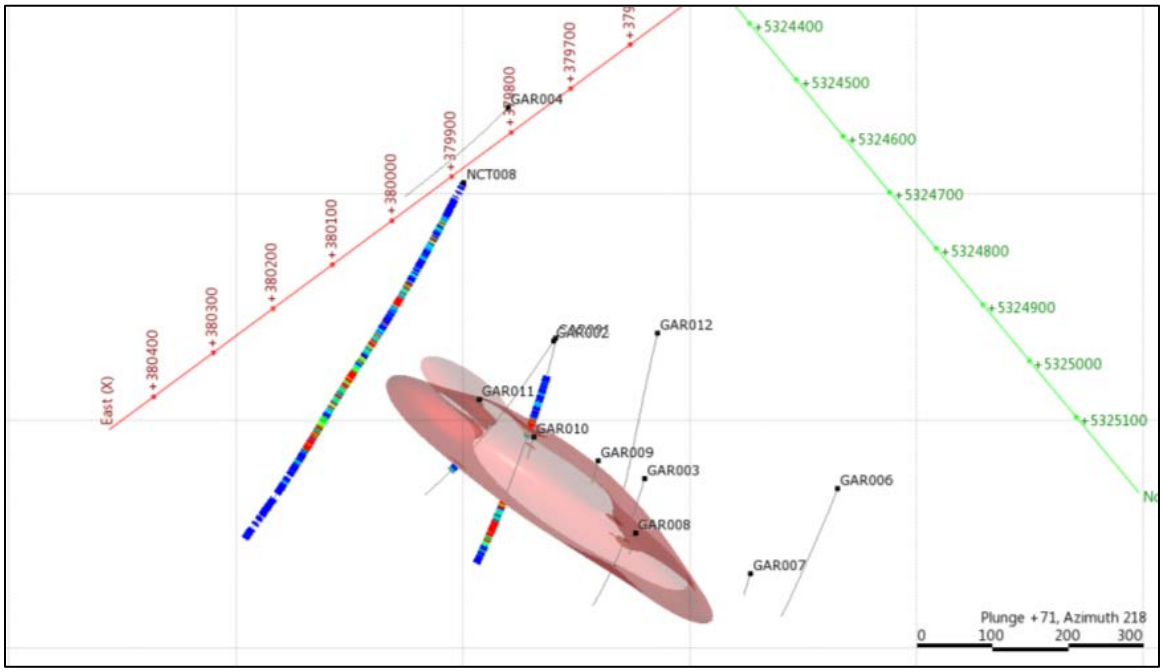

Figure 13. Sulfur assays; blue<0.1%, red>1%. The red shape is Cu>0.1%.

The sulfur assays are not available for all drill holes, but they highlight a pyritic envelope around Garfield (figure 13), which coincides with a short wavelength sericite zone (figure 12).

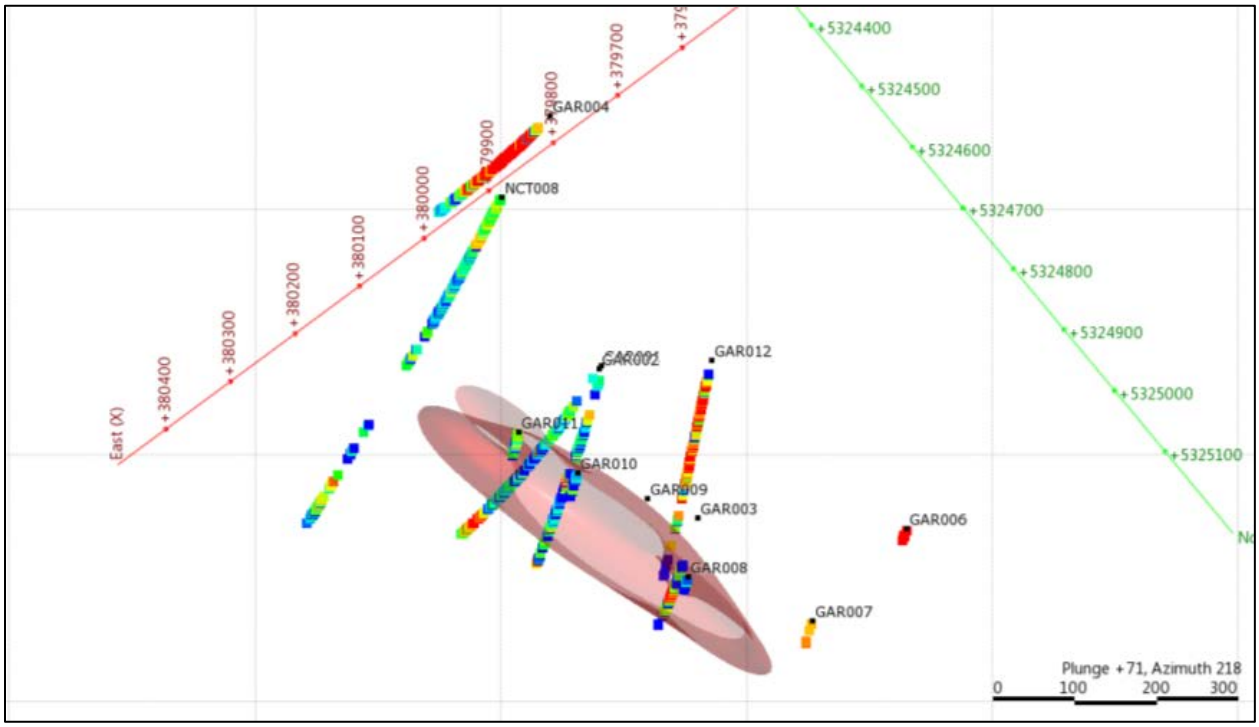

Figure 14. Down hole chlorite compositions; blue<2248nm, red>2258nm. The red shape is Cu>0.1%.

Chlorite compositions also show a distinct zonation, with proximal Mg-rich chlorites and distal Fe-rich chlorite.

Mount Darwin ASD Results

The ASD spectra were classified according to the dominant mineralogy. They were divided into the following categories;

- Biotite
- Sericite
- Chlorite
- Mixed sericite-chlorite
- Kaolinite
- Mixed kaolinite-sericite

Indistinct spectra were flagged as “NULL”.

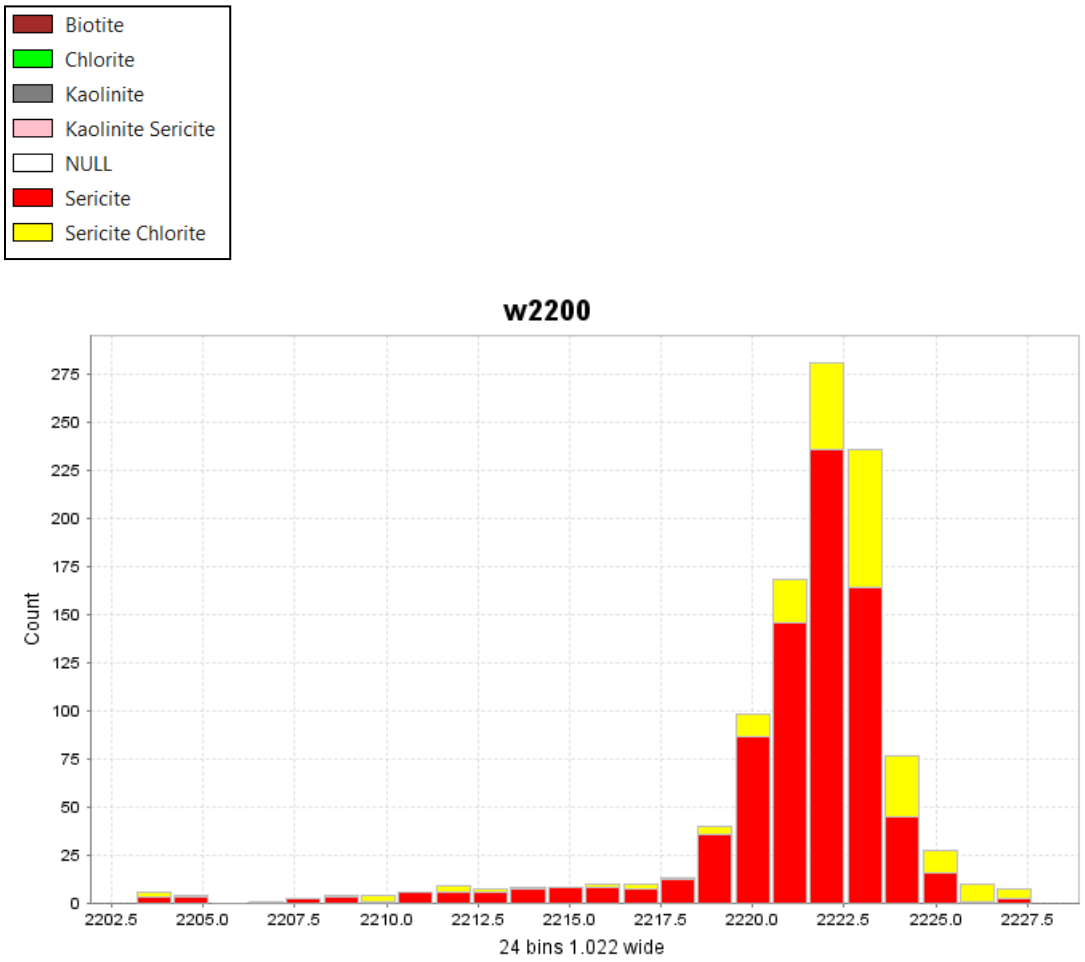

Figure 15. Wavelength at the minimum point of the 2200nm feature for all white-mica bearing spectra from Darwin.

For all the samples containing sericite or sericite-chlorite, the wavelength of the 2200nm feature was extracted and added to a column called “Sericite Composition”. A histogram of these values is shown in figure 15. It is unusual to ever see sericite with wavelengths longer than 2220nm. Very long wavelength micas like this only form in systems where lots of new hydrothermal feldspar is being created. This is a signature of an alkaline hydrothermal system.

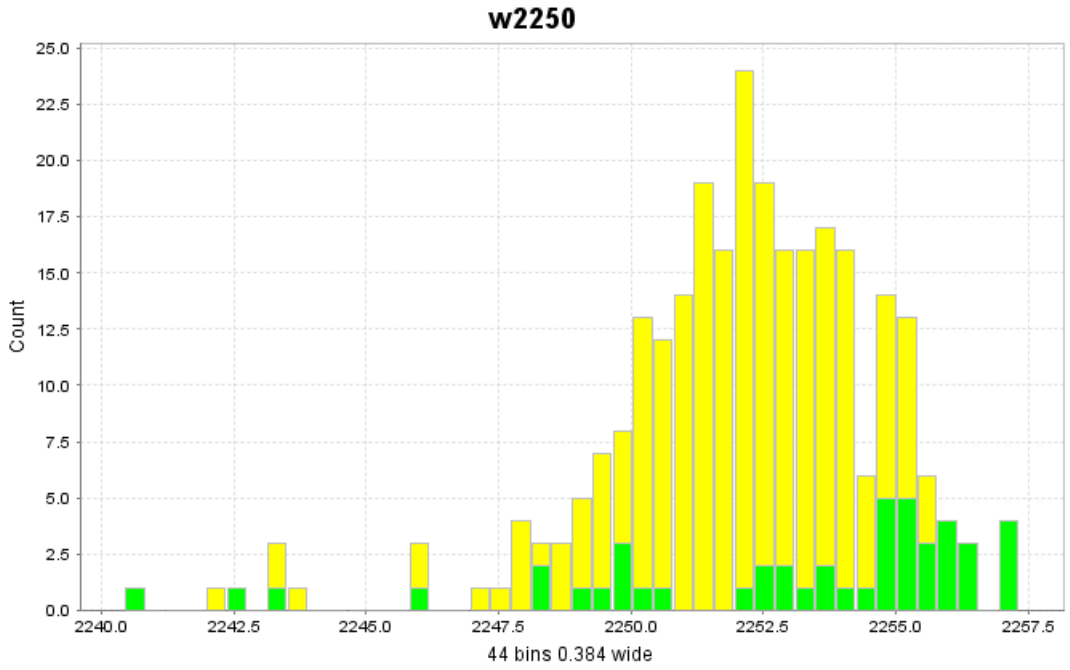

Figure 16. Wavelength at the minimum point of the 2250nm feature for all chlorite-mica bearing spectra from Darwin.

For all the samples containing chlorite or sericite-chlorite, the wavelength of the 2250nm feature was extracted and added to a column called “Chlorite Composition”. A histogram of these values is shown in figure 16.

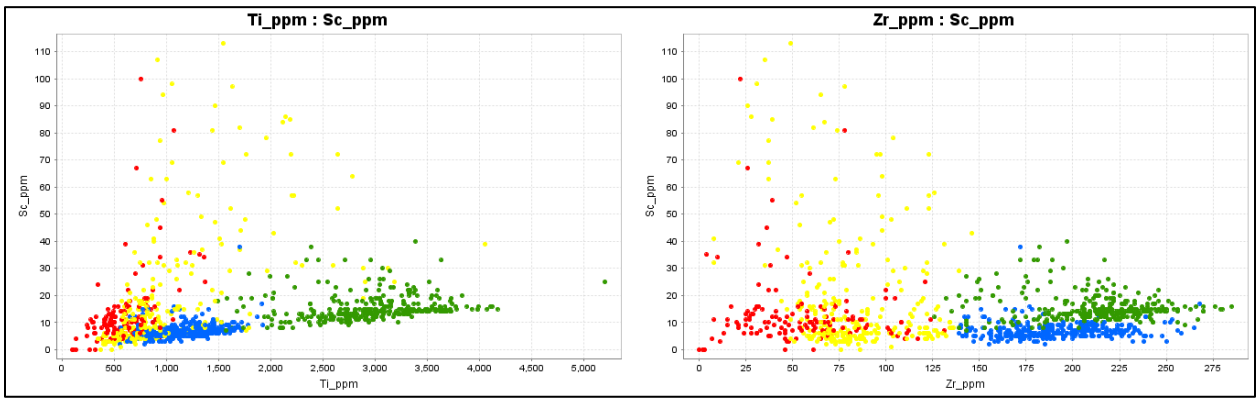

Figure 17. Immobile trace element scatterplots from the South Darwin assay table.

A typical lithogeochemical classification of rocks from an assay file would begin by plotting major elements against silica. In the absence of a SiO2 analysis, one of the most useful elements from picking broad compositional groups is scandium. Scandium is a particularly useful immobile element because it substitutes for Fe into common silicate minerals such as hornblende, pyroxene, chlorite, etc. Sc can be considered as a proxy for the Fe content, but it is much less mobile than Fe during alteration and weathering. As a rule of thumb, basalts will have 30 to 50 ppm Sc, andesites 20 to 30ppm, dacites 10 to

20, and rhyolites less than 10ppm. In the plot above, the green points are broadly a dacitic composition and the blue points are rhyolitic.

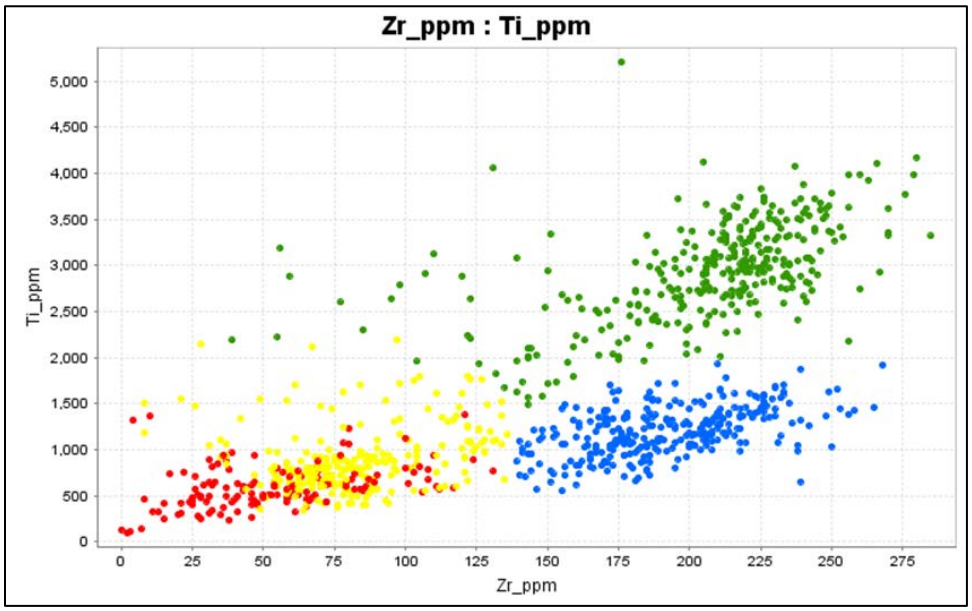

Figure 18. Immobile trace element scatterplots from the South Darwin assay table.

There are two different protoliths, blue and green. The yellow and red groups are altered versions of the blue and green groups, but the distinctions become les distinct as the rocks become more altered. The yellow group has a moderate magnetite content and the red group has LOTS of magnetite. The magnetite is diluting everything else (heading back towards 0,0). It also appears that the alteration is causing localized mobility of Ti and Sc!

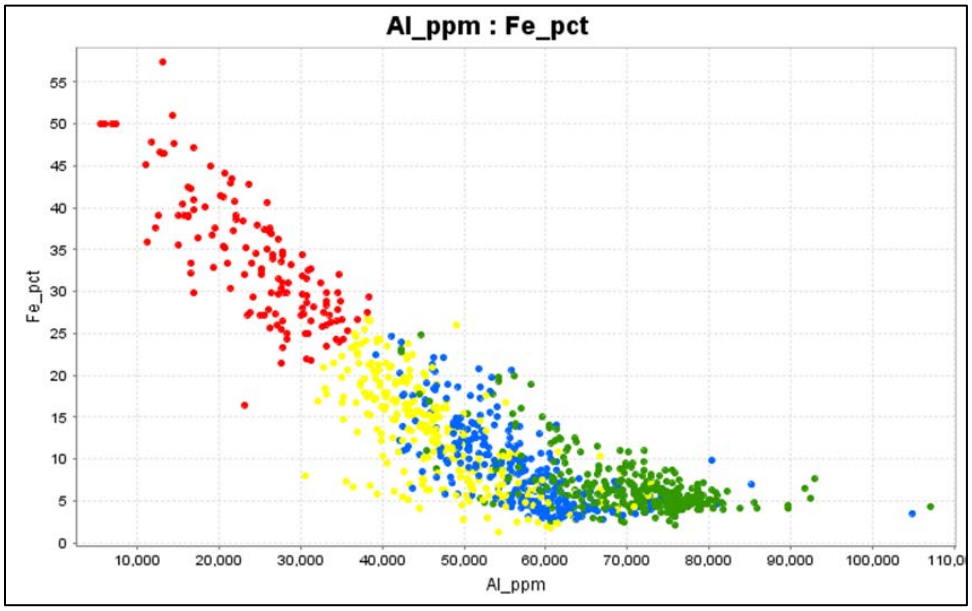

Figure 19. Fe versus Al; The Fe enrichment trend is “diluting” the feldspar content.

Most volcanic rocks have 6 to 8% Al. In mafic rocks the feldspar composition is dominantly plagioclase and in felsic rocks the feldspar composition is dominantly alkali feldspar, but regardless of the rock composition, the feldspar content is about the same. In quartz-rich or carbonate-rich rocks the feldspar content is diluted, so the Al content is lowered. This plot shows the effect of the magnetite addition; Fe increases (more magnetite); Al decreases (less feldspar).

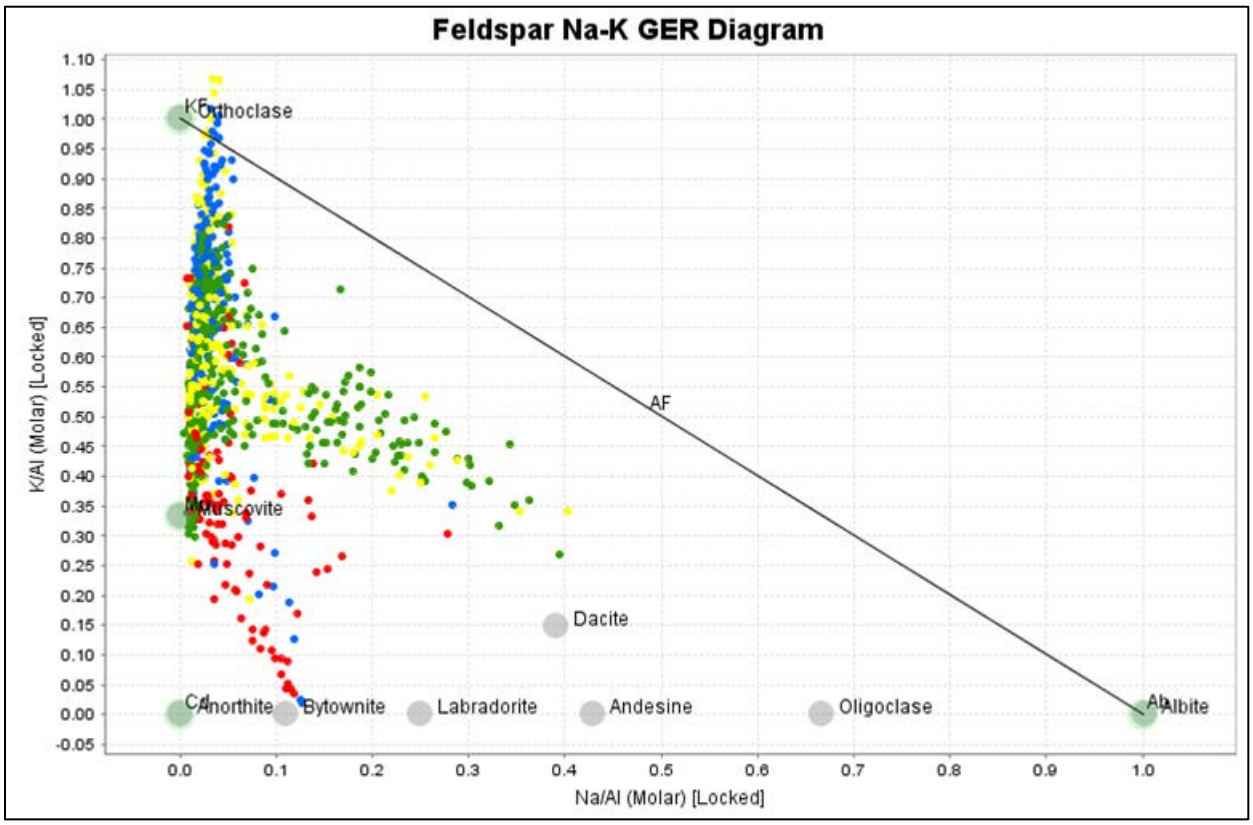

Figure 20. K/Al versus Na/Al molar ratio plot coloured by rock compositions.

Figure 20 above shows a K/Al ratio plotted against a Na/Al ratio calculated on a molar basis. Consider a rock that is totally sericitised. The mineralogy of the rock might be muscovite-quartz-carbonate-pyrite. All of the K and Al in that rock will be within sericite. Muscovite has a composition of $KAl_3Si_3O_{10}(OH)_2$. Therefore the ratio of K:Al in the sericitised rock is 1:3. Similarly, a totally KSpar ($KAlSi_3O_8$) altered rock will have a K:Al ratio of 1:1. In the same way, albitisation can also be tracked. Albite is $NaAlSi_3O_8$: Na:Al =1:1. The projected position of a typical unaltered dacite is shown for reference.

Note that the Darwin rocks are dramatically Na-depleted, but VERY K-rich. The vast majority of points plot well above the projected composition of muscovite therefore must contain an extra K mineral other than sericite. This is KSpar. Also note that the intensely magnetite-altered samples (red) fall below the albite-muscovite tie line. These rocks must have another aluminium bearing mineral, probably chlorite or amphibole.

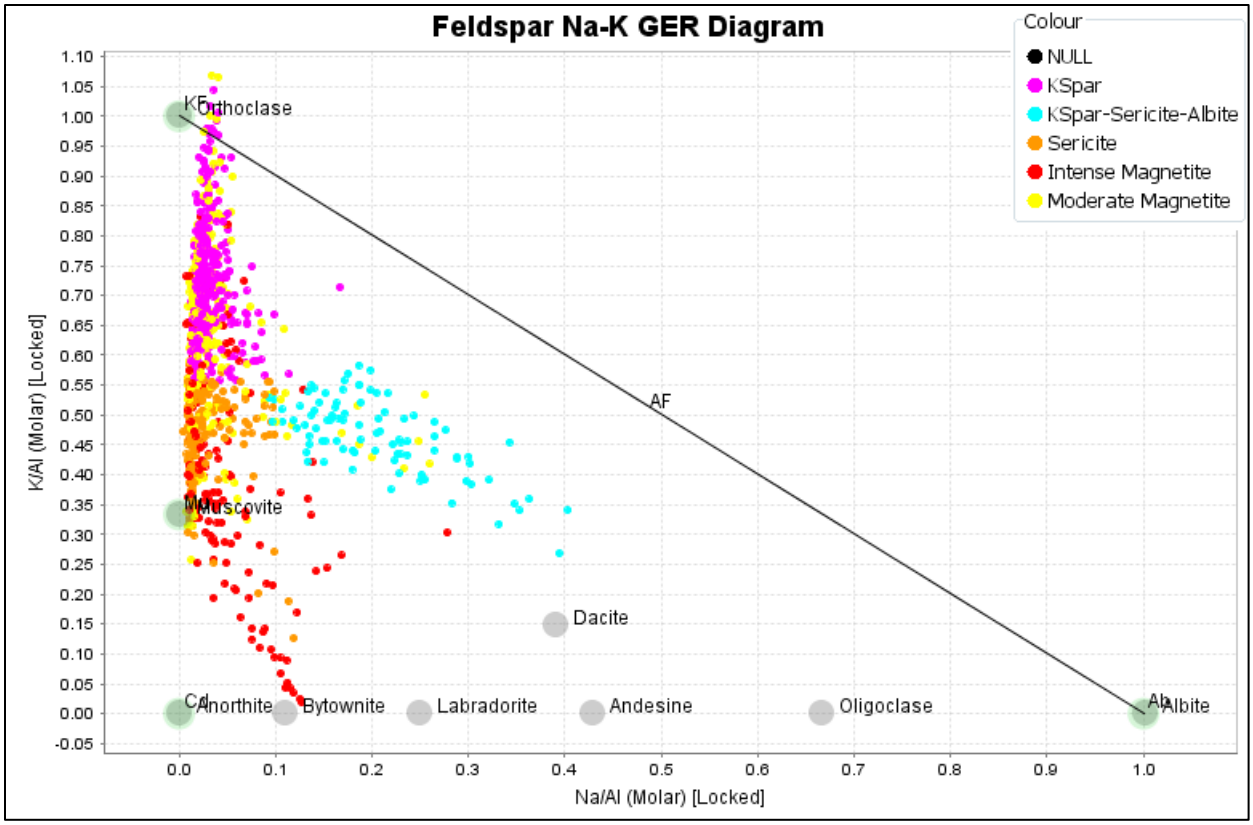

Figure 21. K/Al versus Na/Al molar ratio plot coloured by interpreted alteration.

Rather than plotting rock compositions, another way to look at this data is to use the colours to track alteration (figure 21). The alteration mineralogy has been plotted in terms of 4 components, KSpar, sericite, magnetite and albite. These have been classified using 2 different plots, the K/Al versus Na/Al molar ratio plot, and a K:Al:Fe ternary plot. From the ternary (figure 22), I have picked intense magnetite and moderate magnetite groups, and from the molar ratio plot, the remaining points were classified as KSpar, Sericite, or KSpar-Sericite-Albite groups.

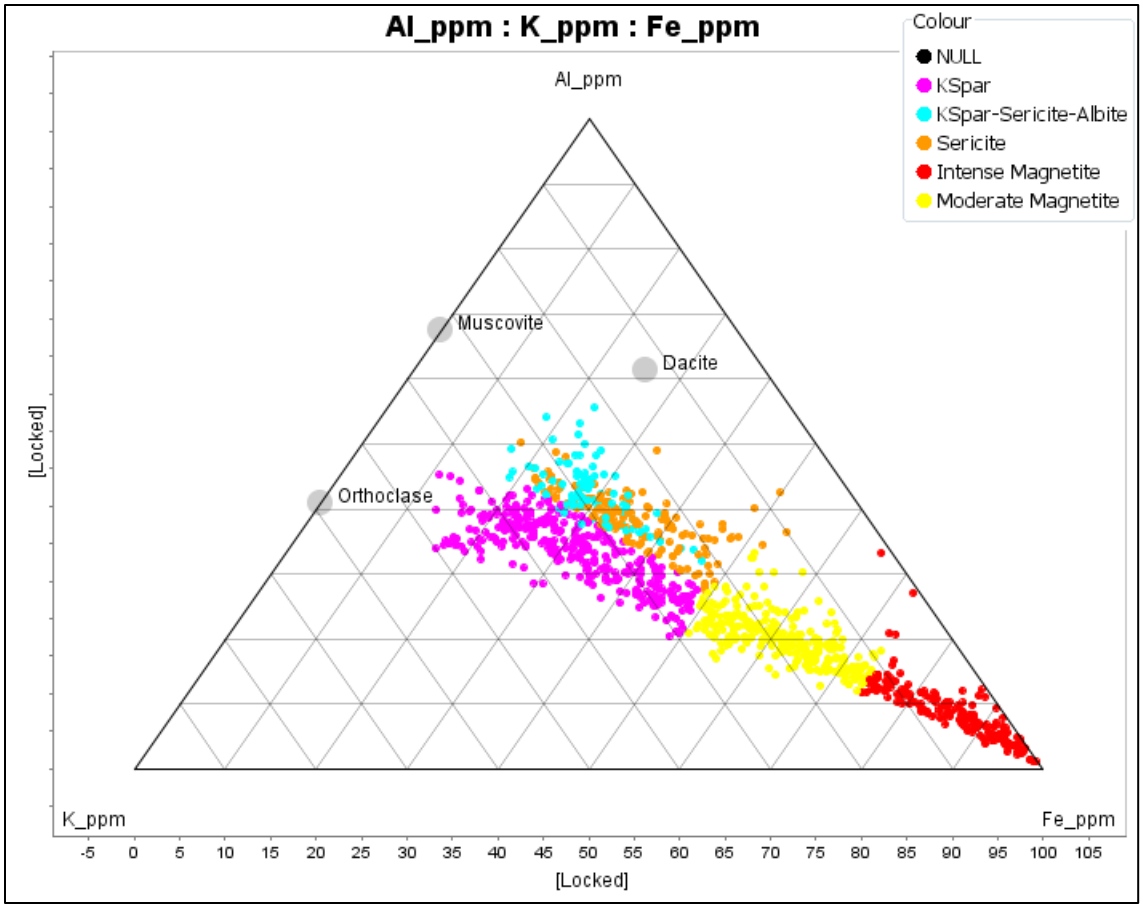

Figure 22. Al-K-Fe ternary plot coloured by interpreted alteration.

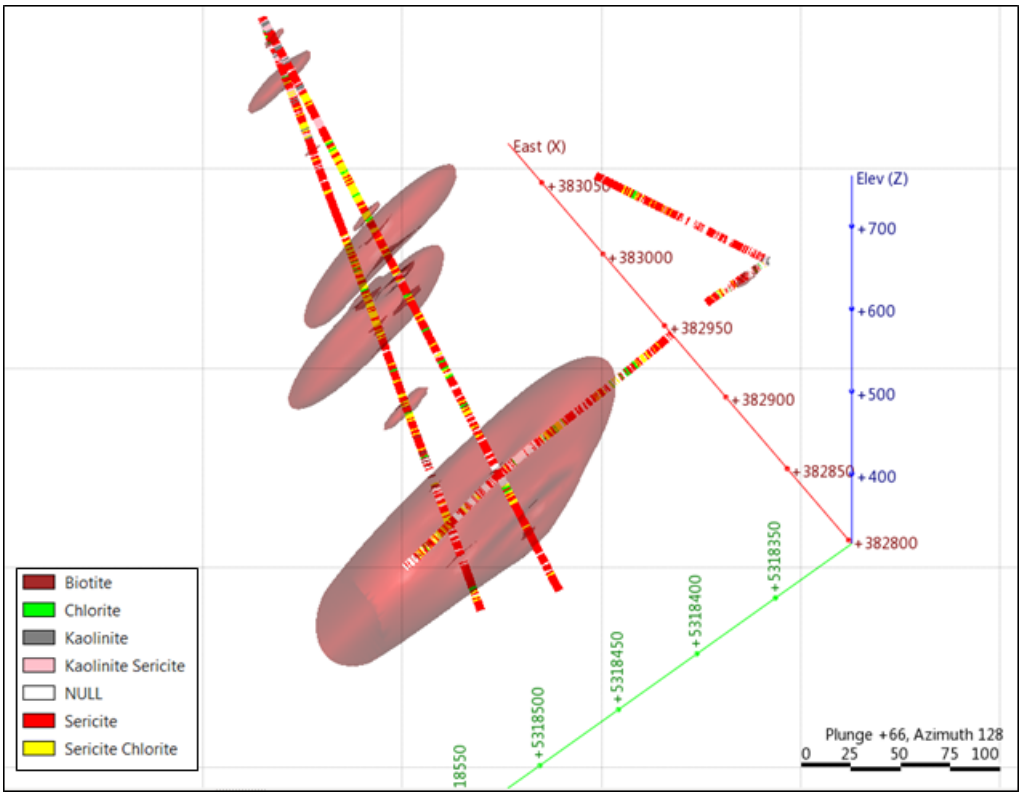

Figure 23. South Darwin drill holes coloured by ASD mineralogy, with a copper grade shell>0.1%.

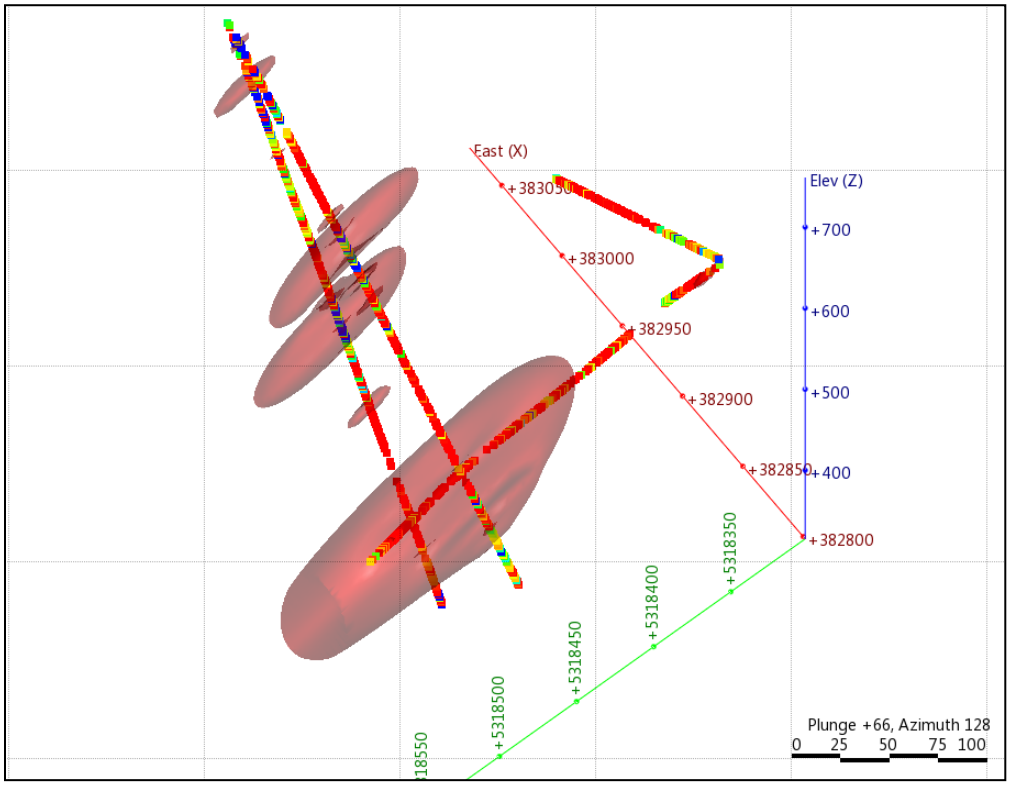

Figure 24. South Darwin drill holes coloured by sericite wavelengths; blue<2216nm red>2222nm.

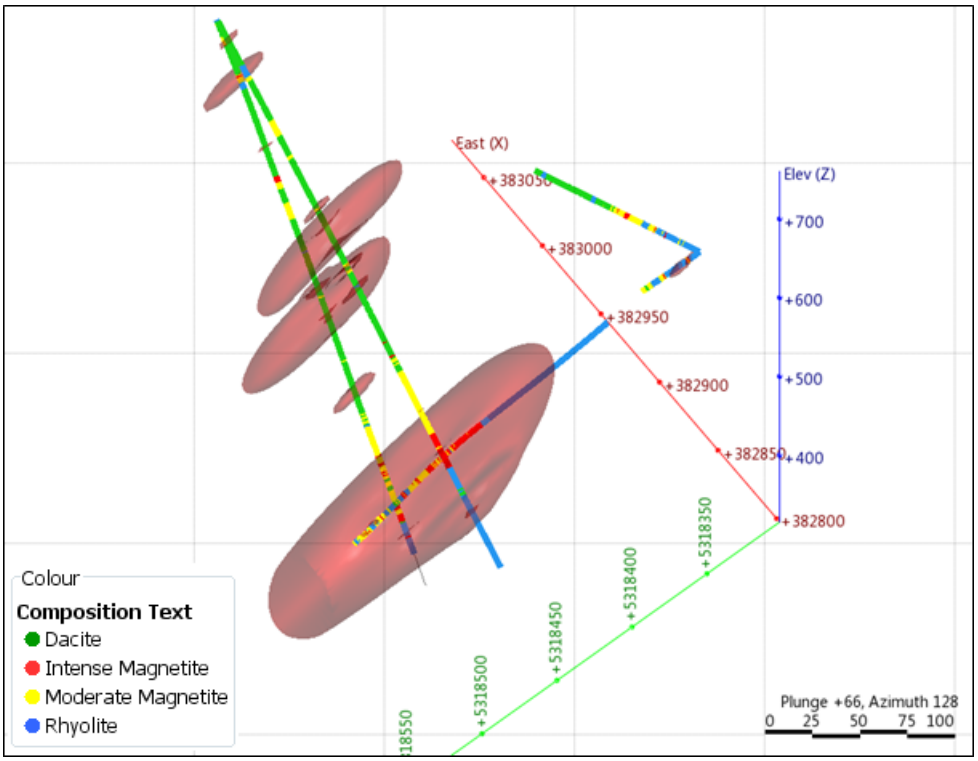

Figure 25. South Darwin drill holes coloured by rock compositions interpreted from geochem analyses.

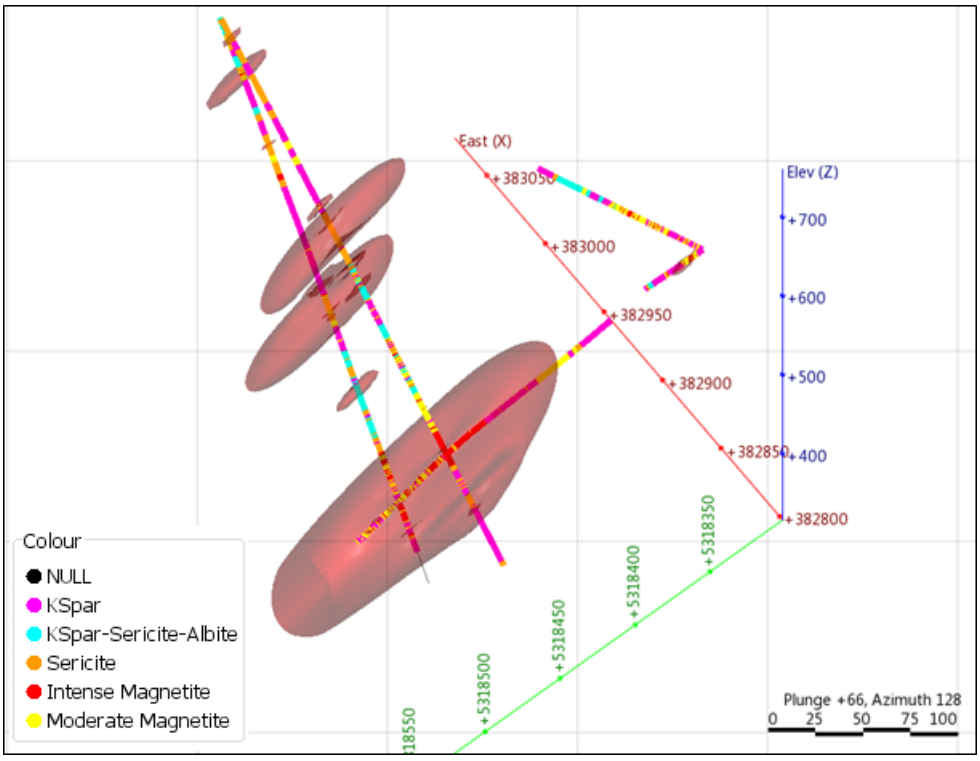

Figure 26. South Darwin drill holes coloured by alteration mineralogy interpreted from geochem analyses.